

Investigation of subsurface structures for the evaluation of hydrocarbon potential using Aeromagnetic Data from Mmaku and its Environs, South-East Nigeria

Ugwu S.A.¹, Nwankwo C.N.², Umeanoh D. C.¹

¹Department of Geology, University of Port Harcourt, Nigeria

²Department of Physics, University of Port Harcourt, Nigeria

Abstract The aeromagnetic map sheet 301 within Latitude $6^{\circ} 00' - 6^{\circ} 30'$ and Longitude $7^{\circ} 00' - 7^{\circ} 30'$ was acquired from the Nigerian Geological Survey Agency. The field data were acquired between 2003 and 2009 by Fugro Airborne Survey Limited and have been pre-processed for diurnal corrections during acquisition with Oasis Montaj software and transmitted as International Geomagnetic Reference Field (IGRF) corrected total magnetic intensity (TMI) in a geosoft grid file format. The acquired TMI values over the study area were digitized with ArcGIS 9.3, processed with OriginPro8 and interpreted using WingLink geophysical software. Qualitative and quantitative interpretations of the study area were carried out and estimate of the thickness of sediments made. Fast Fourier transformation were performed over the gridded data and a plot of the energy versus frequency (cycle/m) for each of the 16 cell divisions were generated, giving the thickness of sediments as the average of the maximum and minimum half slope values. The lineament map shows the major linear structures trending NE-SW direction and the minor ones trending NW-SE direction. The major trend direction conforms to the trend of the Benue Trough. Five dominant magnetic units were identified which fall into three main groups-the high, medium and low magnetic anomalous zones. Inspection of the map shows an intrusive rock of large extent containing magnetite at the central part of the map and a dyke of very low magnetic values at the east and north. The medium magnetic anomalous unit is located at the westerly part of the map. A fold axis or fault trending NE was inferred from the map where the contours are parallel to sub-parallel to each other. The average estimated depth across the entire area is about 7 km.

Keywords Aeromagnetic, lineaments, magnetic anomalies, structures

Introduction

Aeromagnetic data has been a very useful geophysical investigation tool especially in mapping magnetic basement in sedimentary rocks and delineating igneous bodies within sedimentary sections as well as locating lineaments and structures which could be possible host to varying earth resources including groundwater. Apart from basement-related problems, the magnetic method has expanded as a tool for finding iron ore to a widespread tool used in exploration for minerals, hydrocarbons, ground water, and geothermal resources. The method has also been found useful in supplementary applications which [1] listed to include studies focused on water-resource assessment [2-3], environmental contamination issues [2], seismic hazards [3-5], volcano related landslide hazards [6], locating buried pipelines [7], archaeological mapping [8], and delineating impact structures [9-10], which can sometimes be of economic importance.

One of the major uses of aeromagnetic method has also been for the estimation of depth to basement and thickness of sediments within sedimentary basins. Although the method was used in mapping igneous and metamorphic rocks and structures related to them because these rocks have high magnetization compared to other rocks [11-12], improved high resolution technology flown closer to the ground and with narrower spacing,



has made aeromagnetic surveys presently designed to view subtle magnetization contrast than has been targeted [1, 13].

In recent times, researchers have worked on the Lower Benue Trough using aeromagnetic, gravity and other geophysical methods. However, there has not been sufficient detailed aeromagnetic study and reports in vast part of Enugu including Mmaku and its adjoining parts of Udi. Most works on the area have been limited to basic geological mapping of outcrops and other geophysical mapping including vertical electrical sounding and electromagnetic investigation for groundwater. This study aims at establishing the local depth of sediments around Mmaku and its adjoining parts of Udi covered within the aeromagnetic map sheet with a view to understanding the aquifer and hydrocarbon potential of the area.

Oyebuchi [14] pointed out that in most sedimentary basins, magnetic anomalies arise from secondary mineralization along fault planes which are often revealed on magnetic maps as surface linear features. The primary measurement taken in magnetic survey is the magnetic susceptibility of rocks which is a measure of the inclination of magnetic minerals in rocks to the earth's magnetic field. The total magnetic intensity (TMI) often shown on aeromagnetic maps is a measure of total magnetization of magnetic minerals in rocks.

Geology of the Study Area

The study area covers the entire Nigerian map sheet 301 and it is located in Enugu state and parts of Anambra state, south-east Nigeria. The area falls within the Lower Benue Trough with the coordinates of Latitude $6^{\circ}00' - 6^{\circ}30'N$ and Longitude $7^{\circ}00' - 7^{\circ}30'E$ (Fig. 1). The Lower Benue Trough has somewhat developed different tectonic history resulting in the formation of the Anambra Basin to the west and Abakaliki Anticlinorium to the east [15]. According to Murat [16] reconstruction model, the Anambra Basin remained a stable platform supplying sediments to the Abakaliki depression during a period of spasmodic phase of platform subsidence in the Turonian. Following the flexural inversion of the Abakaliki area during the Santonian uplift and folding, the Anambra Basin was initiated.

The five main formations within the study area are Nkporo Shale Formation, Mamu Formation, Ajali Formation, Nsukka Formation and Ameki Formation. The ages of the formations range from Maastrichtian to Campanian and to Eocene (Ameki Formation). From the re-digitized map sheet 301 in figure 1, the formations become younger towards the SW.

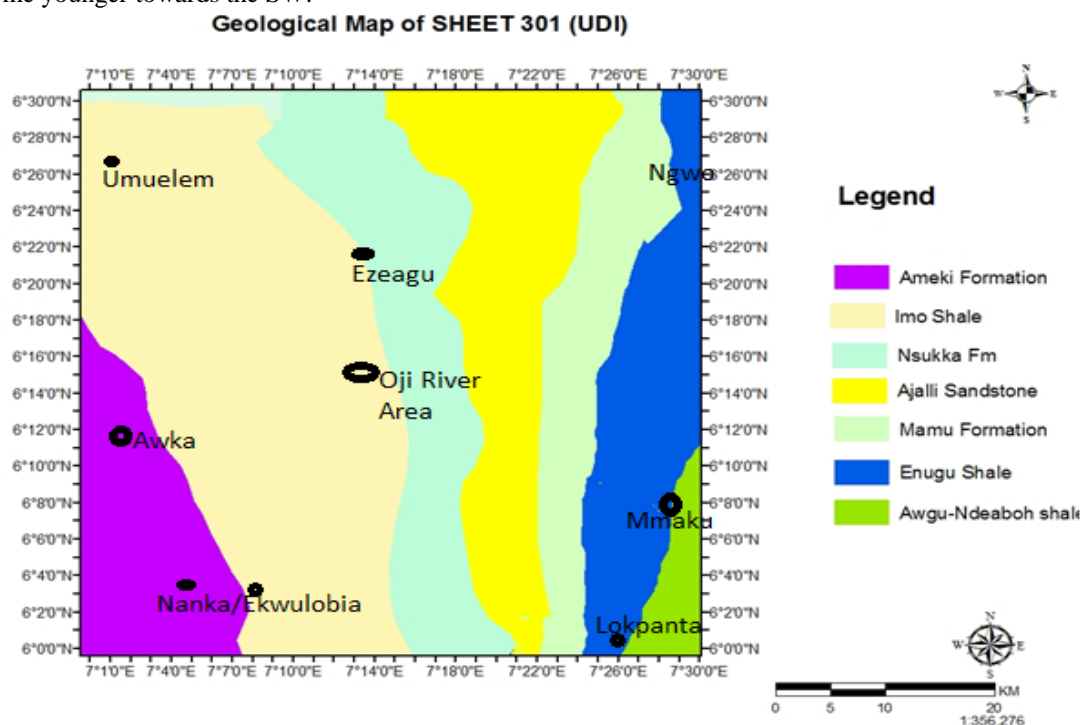


Figure 1: Geologic Map of the Study Area (Modified Sheet 301 and Re-digitized NGSA geologic map of Nigeria)



Processing of the Aeromagnetic Data

The airborne magnetic data were made available by the Nigerian Geological Survey Agency (NGSA), Abuja on request for academic research purposes. The raw data had been pre-processed using Oasis Montaj software and corrected *in-situ* for diurnal corrections by the NGSA and was transmitted as International Geomagnetic Reference Field (IGFR) corrected TMI in geosoft grid file format. Reduction to the pole at low latitude was applied to the upward continued gridded TMI file. This as an important filtering process in magnetic data recalculates the total magnetic field intensity as if the inducing magnetic field is at 90° inclinations thereby transforming dipolar magnetic anomaly to mono-polar anomalies centered on their causative bodies, hence making interpretation simpler.

Materials and Methods

The data used for this study was acquired from an airborne survey flown in Nigeria between 2003 and 2009 at flight line direction NW-SE and at flight line spacing of 500 meters. The terrain clearance was at low altitude of 80 meters while the tie line spacing was 2 km at flight line direction of NE-SW. The remote sensed geophysical data includes aeromagnetic, radiometric and limited electromagnetic data.

The raw data was pre-processed using Oasis Montaj software by the NGSA and was transmitted as IGFR corrected TMI saved as geosoft dataset in geosoft grid file format. The IGFR provides the means of subtracting on a rational basis the expected variation from the main field to leave anomalies that may be compared from one survey to another, even when surveys are conducted several decades apart and when, as a consequence, the main field may have even been subjected the secular variations [17].

Digitization was done in grid of 1km x 1km spacing and values of TMI and coordinates were picked at the intersection of the grid nodes. This 1km x 1km grid points generated over 6000 sample points. The x and y show the coordinates while the z represents the TMI value at the point. The coordinates were automatically converted and recognized in meter scale. This was implemented by ArcGIS 9.3 software and the xyz data was saved as MS Excel file format.

WingLink, OriginPro8, MS Excel and Surfer10 software were employed for the manipulation, presentation and interpretation proper. Major aspect of the processing and filtering of the data was implemented with WinGLink geophysical interpretation and visualization software. The filtering was aimed at enhancing the data for qualitative and structural interpretation.

Regional anomaly field is the magnetic anomaly component with long wavelength (low frequency) and which represents deep-seated bodies. This corresponds to the low pass filters and is accomplished through upward continuation. The residual anomaly on the other hand is the short wavelength anomaly (high frequency) which is left after removal of the regional. The residual anomaly is a field which corresponds to the high pass filters and is indicative of local trend variations giving clues on structures for possible mineral or ore emplacement. Therefore, data interpretation of aeromagnetic map is based usually on the residual magnetic field:

Residual field = total field – regional field.

This project found that a 10x10 kilometer window (cells or grids) was useful for basement depths encountered. After the average radial (Energy) power spectrum is calculated using Fast Fourier Transform, it is plotted in MS Excel as Log of Energy (FFT magnitude) versus radial frequency in Cycles/sec. A straight line is then visually fit to the energy spectrum, usually in the higher frequency of the figure. The negative slope of this line is equal to twice the depth to the centre of mass of the bodies producing the magnetic field. After the depth has been calculated over one window, a new calculation is made over a new window. This continues over the grid until all windows have their radial spectra calculated and the depths picked. Depth values picked are believed to be at the centre of the grid and represent depth to top of magnetic body.

After separation of the magnetic data into 16 windows of 10km x 10km for spectral depth analysis, the data was imported into Microcal OriginPro8 software for scientific data analysis and processing. The FFT was performed using the FFT function in the data analysis tool after the data was smoothed in OriginPro8 using smoothing function. The FFT function was used to separate the TMI data of the windows (called cells) into their frequency component and energy (FFT magnitude or the absolute value of the FFT complex) spectrum.



Results and Discussion

The raster map (Fig. 2) of map sheet 301 was obtained from Winglink software. The raw data (in geosoft format) was first opened with ISRI ArcGIS software before opening in Winglink. The raster image simulates colouring of magnetic intervals between contour lines. The colour ranges are taken from the natural light spectrum: red (high), orange and yellow (medium) and green and blue (low). These raster permits easy identification of causative magnetic bodies through the entire map. So at a glance, one identifies the magnetic highs and lows. Using a contour interval of 10nT, the map was reproduced to give the TMI contour map of Figure 3.

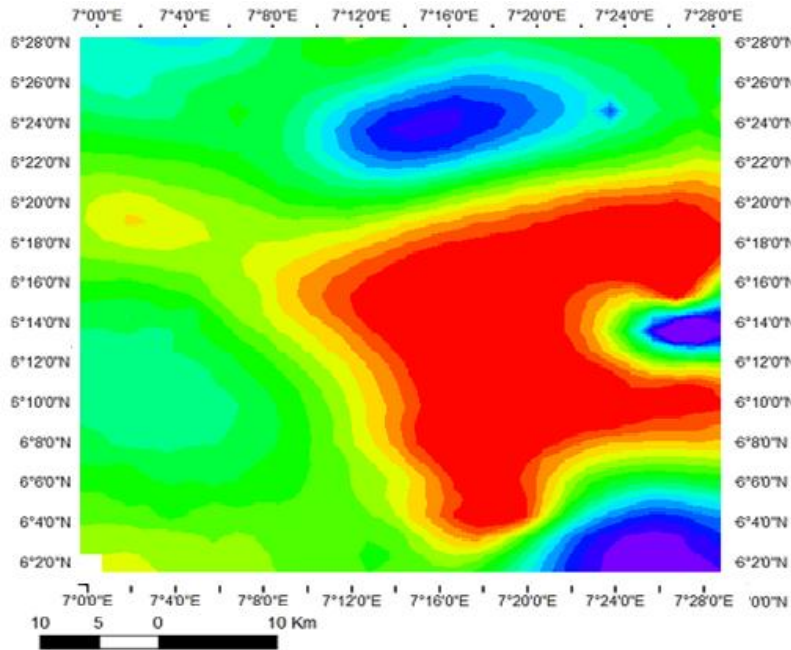


Figure 2: Raster Map of the Aeromagnetic Data (Udi Sheet 301)

This magnetic contour map provides clue to the variation of the total magnetic intensity within the area. It also helps an analyst to partition the area into its various magnetic zones (labelled 1 to 5; Fig. 3). The profiles taken through the area is based on the anomalies established by the contour maps. The magnetic contouring also allows for the production of the magnetic basement topography, the first vertical derivative and the residual contour maps.

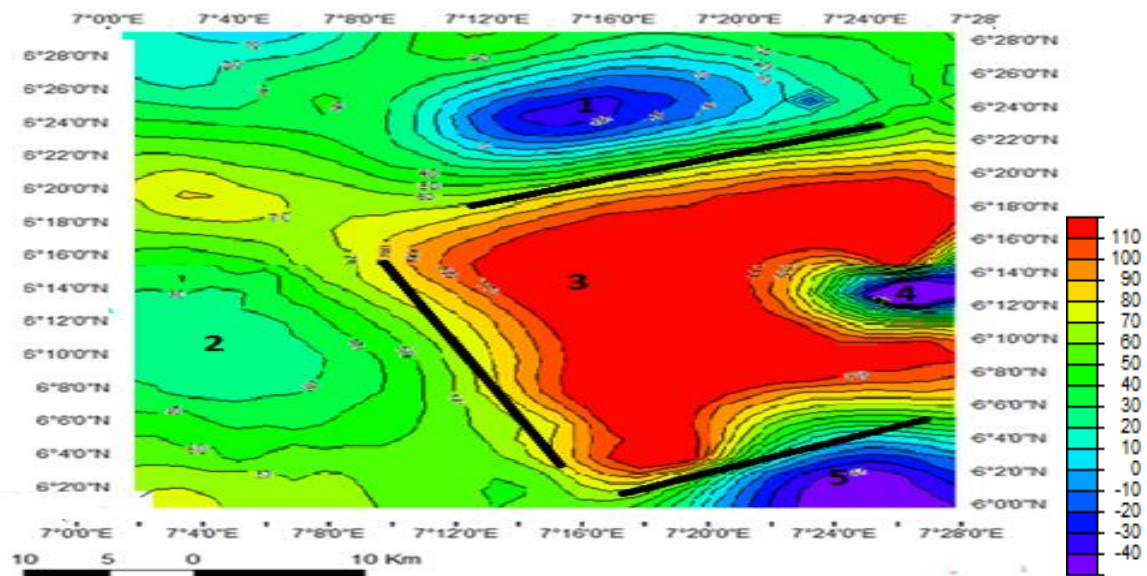


Figure 3: Total Magnetic Intensity (TMI) Contour Map (in nanotesla)

The magnetic topography of the study area based on the above TMI contour map is shown in Figure 4. At a glance, the areas of highs, lows and medium magnetic anomalies are observed from the magnetic topographic map.

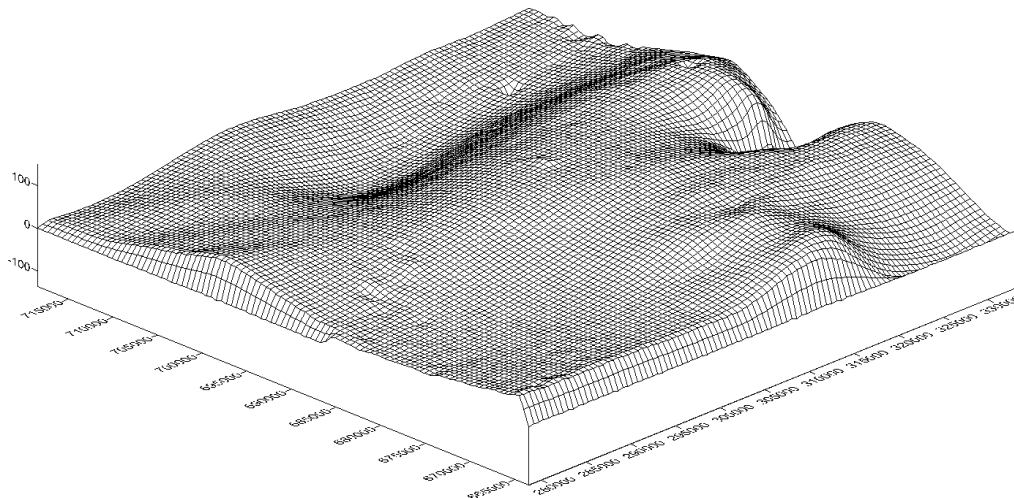


Figure 4: Magnetic Topography of the Study Area

Similarly, Figure 5 is the produced regional magnetic anomaly map showing the dominant trend of NNE-SSW which is common to the Pan-African Orogeny. While the first vertical derivative (Fig. 6) gives the very shallow source, the residual contour map (Fig. 7) gives the map of the magnetic values after separation of the regional from the observed anomalies. The TMI (magnetic contour) map as well as the residual map was subjected to qualitative interpretation.

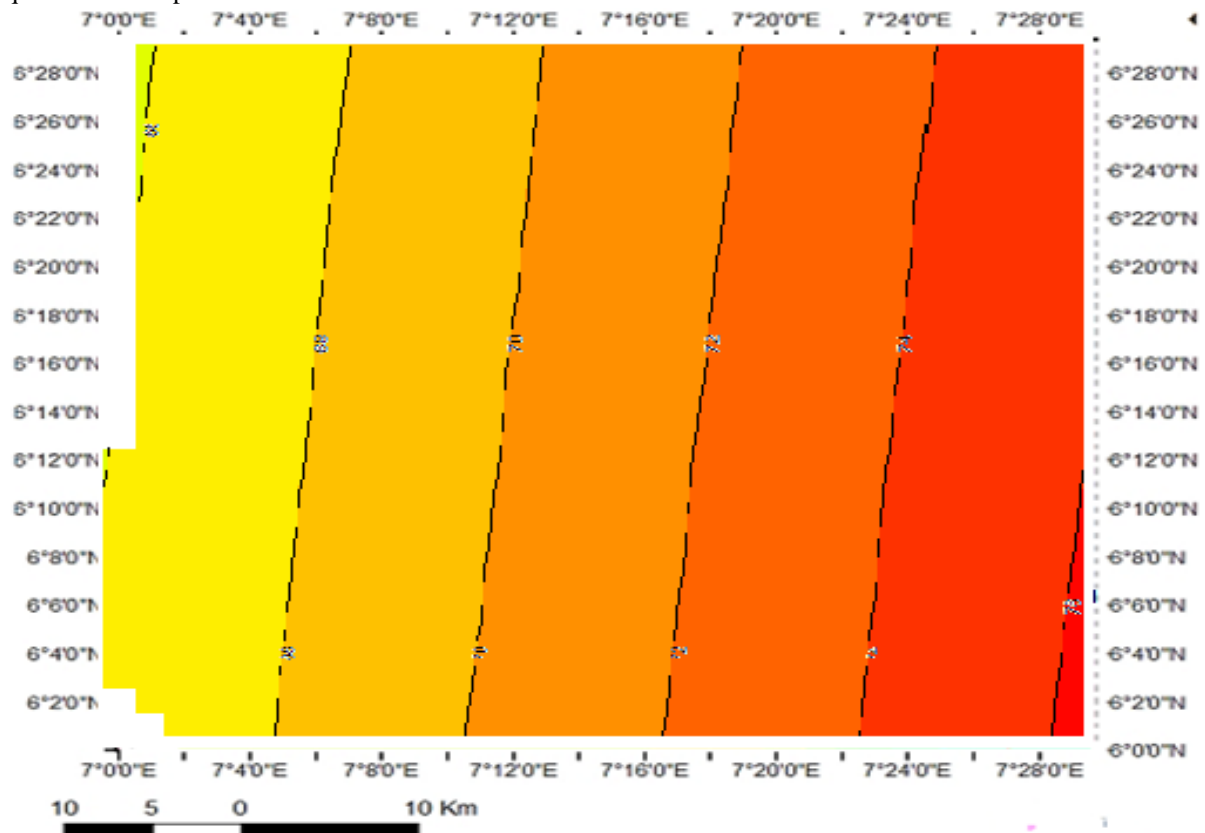


Figure 5: Regional Magnetic Anomaly Map

Figure 8 is the same residual magnetic map with profiles and locations across the anomalous units.

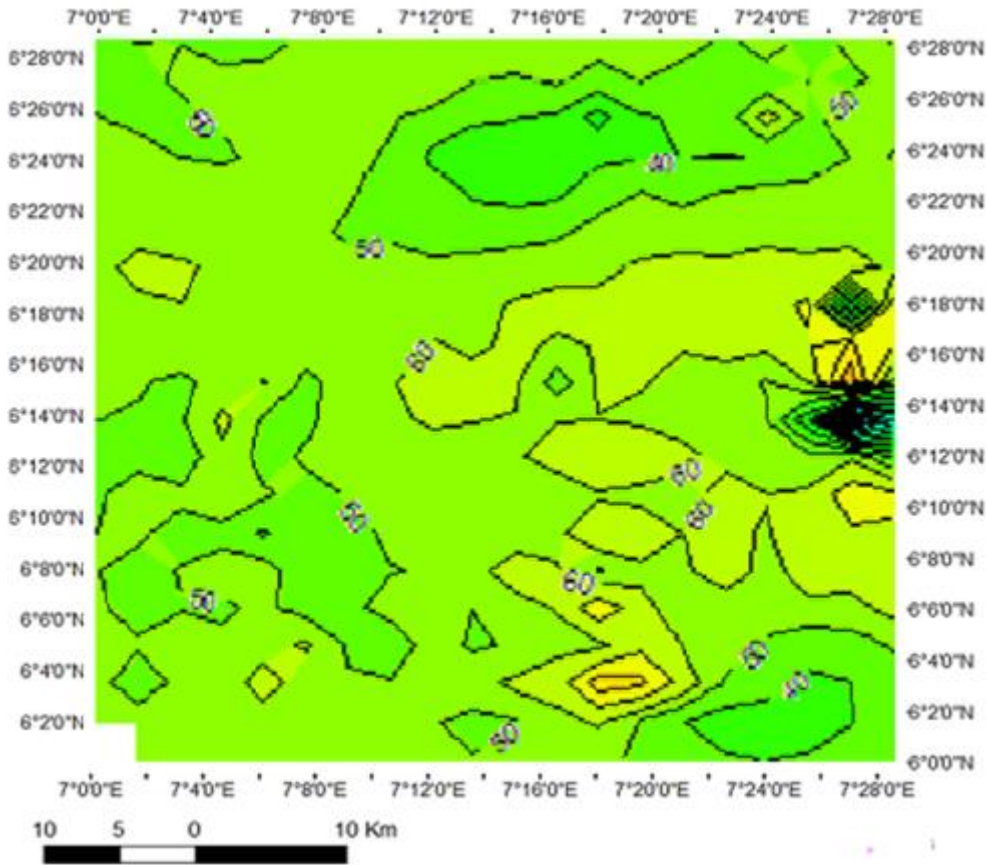


Figure 6: First Vertical Derivative Anomaly Map

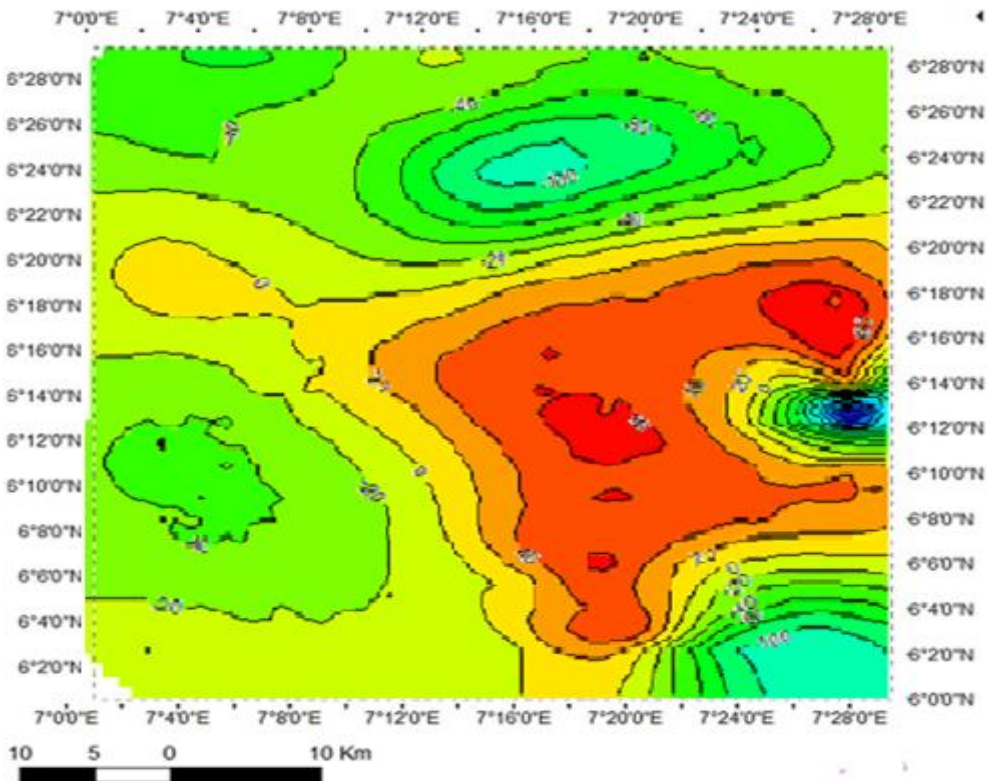


Figure 7: Residual Anomaly Map (legend values in nT)

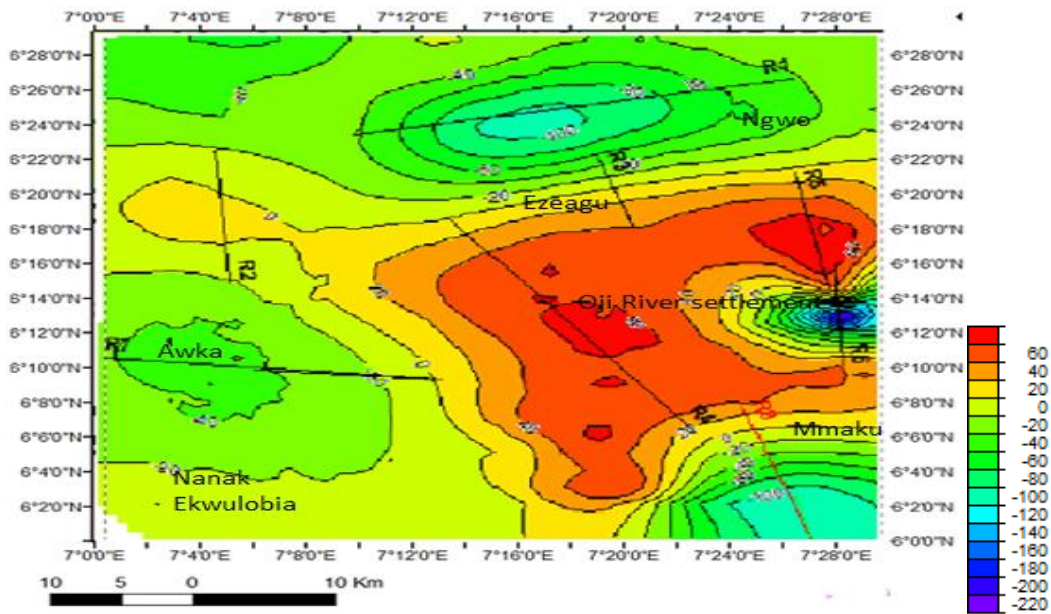


Figure 8: Residual Anomaly Map with Profiles and Locations

By visually inspecting the total magnetic intensity and residual anomaly maps, the linear structures were taken and the lineament map (Fig. 9) generated. The linear structures include all the observed features on the aeromagnetic map with a linear path ascribing the long axis. From the map, most of the lineament structures trend NE-SW while few others trend in the NW-SE direction. This enhances interpretation of the geologic events in the area better.

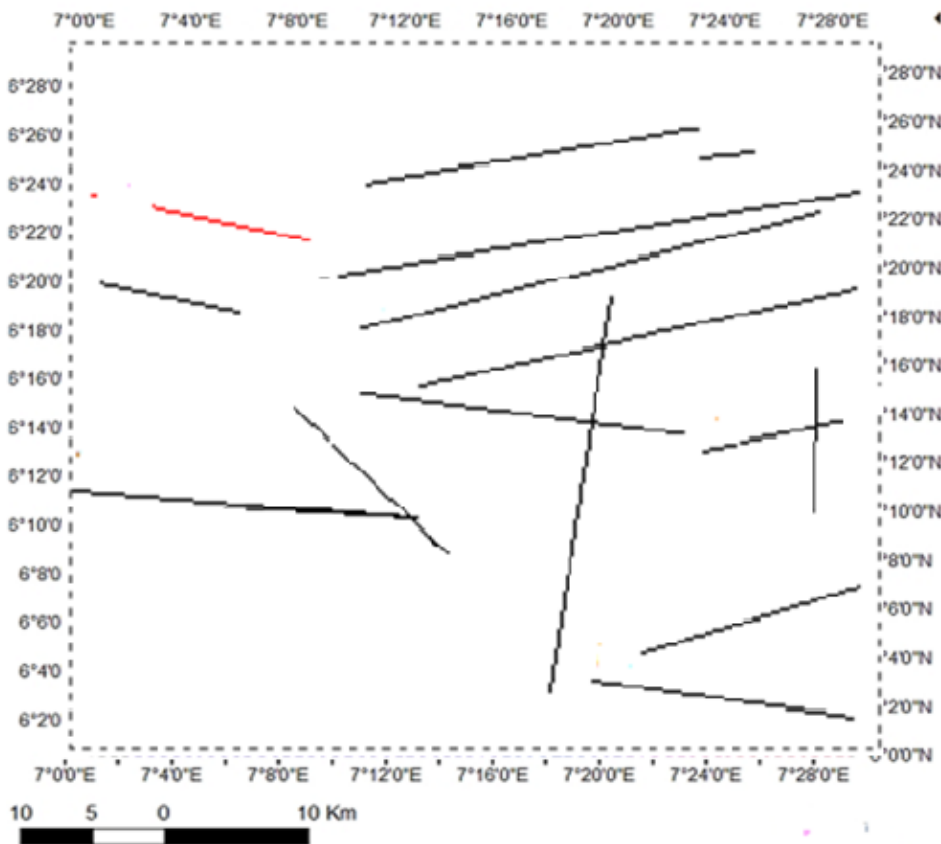


Figure 9: Lineament map through the study area

While qualitative interpretation provides the foremost information about the study area by inspection of the various magnetic maps, quantitative interpretation is achieved through spectral depth analysis. It established the local depths to the magnetic basement. The spectral analysis in this study was done in a 16 cell grids within the aeromagnetic map.

Table 1 is depth computation results based on the plotted data of LogE vs radial frequency (cycle/meter) on each of the cells [18]. The table shows the maximum and minimum slopes (S1 and S2) with their corresponding maximum and minimum depth values (D_{max} and D_{min}) respectively to the magnetic sources across the study area. The equation of the graphs can be related to the equation 1:

$$[\text{Log } Y = (c_1 - c_2) - (m_1 - m_2) x] \tag{1}$$

where c_1 and c_2 are the intercepts along y-axis, m_1 and m_2 are the slopes.

The slope is a negative one; hence the corresponding depth values are all negative values. Figures 10 to 15 are representatives of the various plotted energy-frequency profiles.

Table 1: Slope and Depth Computation through the Cells

Cell plots	Maximum Slope (S1)	Minimum slope (S2)	Maximum Depth $d_{max} = S1/2$	Minimum Depth $d_{min} = S2/2$
C1	-15613.33	-2865.59	-7806.66	-1432.80
C2	-18307.65	-3651.09	-9153.82	-1825.55
C3	-25639.18	-4268.83	-12819.59	-2134.42
C4	-20853.35	-1850.51	-10426.68	-925.25
C5	-14405.64	-3466.69	-7202.82	-1733.34
C6	-24219.00	-5123.00	-12110.00	-2562.00
C7	-21641.93	-10820.97	-7942.54	-3971.27
C8	-22056.25	-3449.65	-11028.12	-1724.83
C9	-24636.83	-4754.78	-12318.42	-2377.39
C10	-24484.02	-4161.12	-12242.01	-2080.56
C11	-22055.01	-4275.49	-11027.51	-2137.74
C12	-27149.00	-6025.66	-13574.50	-3012.83
C13	-23670.11	-3939.58	-11835.06	-1969.79
C14	-20661.20	-4341.69	-10330.60	-2170.85
C15	-22433.18	-3742.68	-11216.59	-1871.34
C16	-25072.95	3899.56	-12536.47	-1949.78

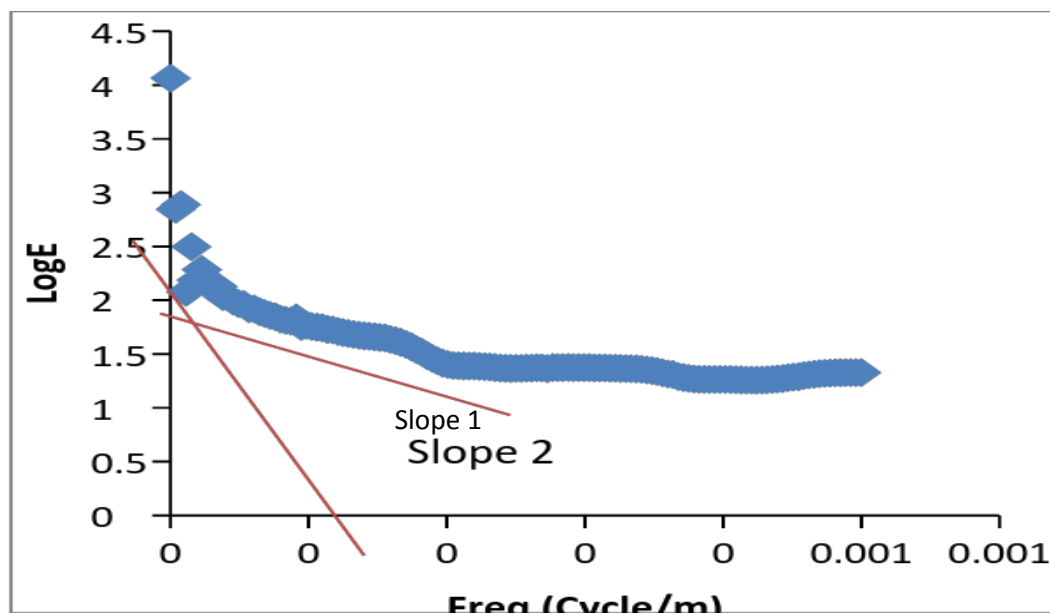


Figure 10: Plot of LogE vs Frequency of Cell 1 Parameters



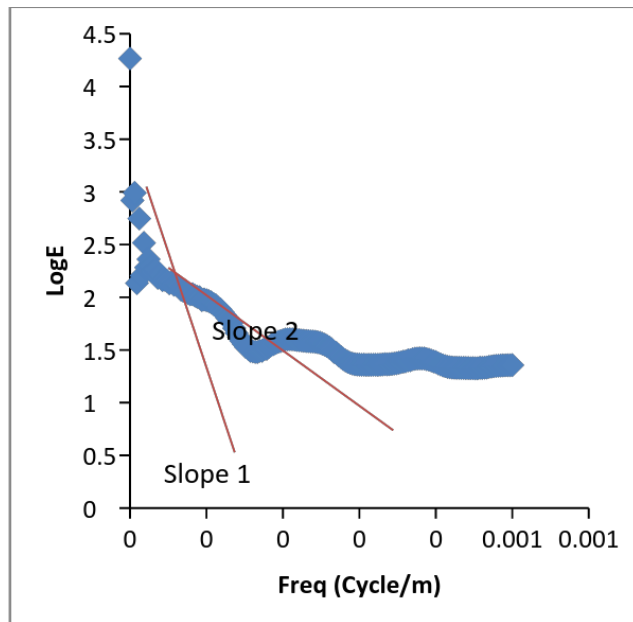


Figure 11: Plot of LogE vs Frequency of Cell 2 Parameters

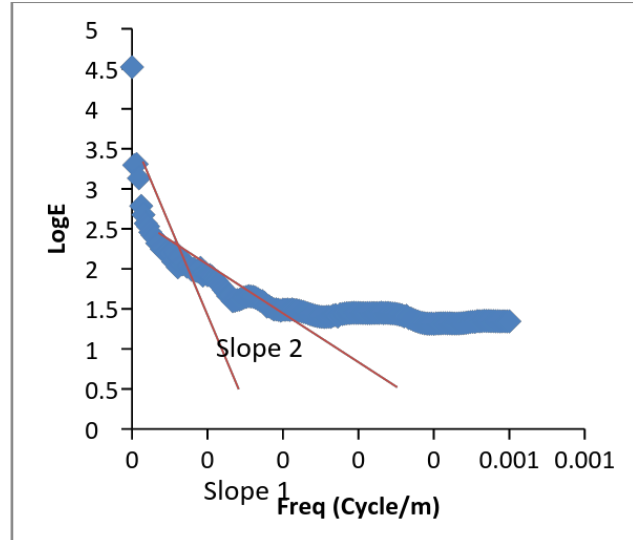


Figure 12: Plot of LogE vs Frequency of Cell 3 Parameters

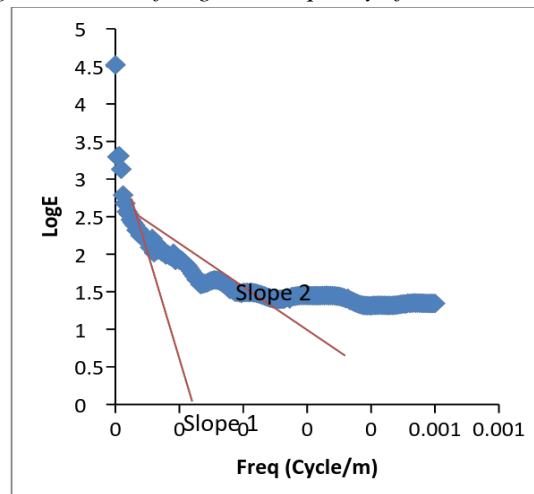


Figure 13: Plot of LogE vs Frequency of Cell 4 Parameters

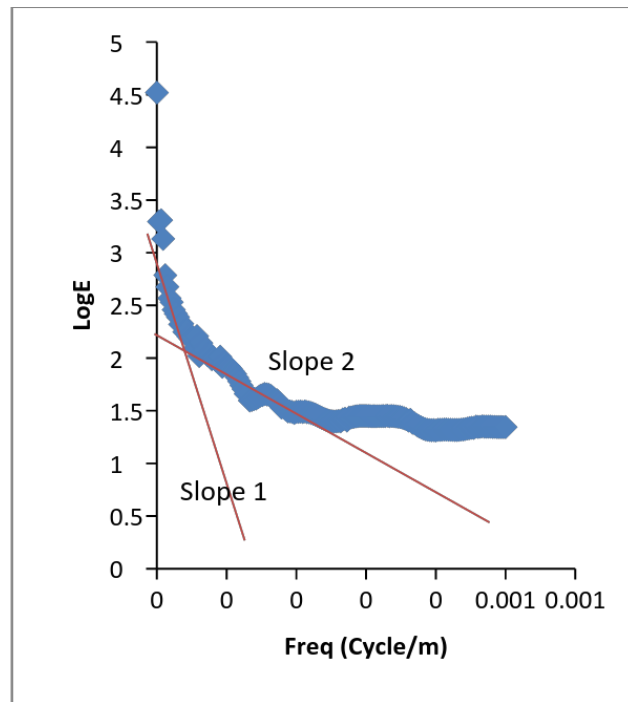


Figure 14: Plot of LogE vs Frequency of Cell 5 Parameters

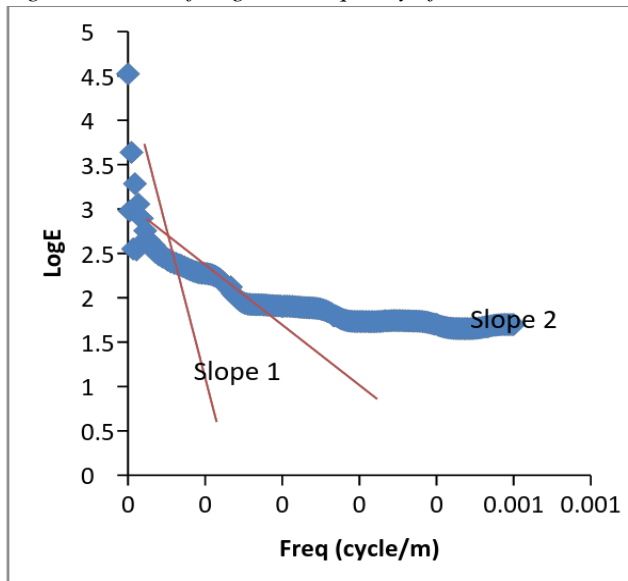


Figure 15: A Plot of LogE vs Frequency of Cell 6 Parameters

Interpretations

Qualitative interpretation methodology involves the inspection of the aeromagnetic data (residual anomaly map, Fig. 7) on the computer screen or on the printed hard copy with a view to identifying and defining the boundaries of magnetic units, as well as structures affecting the shape of the magnetic units. Figure 7 shows the local anomalous variation of the shallow features after removal of the regional field. The contour lines help to provide the shape, direction of linear structures and the causative source bodies which may characterize ore minerals emplacement or reservoir structures. In other to accurately refer to these anomalous bodies, profiles were taken on the residual maps through them. Considerations were also given to other enhanced maps for accurate understanding of the structural architecture of the study area.

By visual examination of figures 3 and 7, five dominant magnetic units can be identified which fall into three main groups - the high, medium and low magnetic anomalous zones. The major and only high magnetic source body is located at the central part of the map and it is a very large magnetic unit. It extends from the north



central to the NE, South and western parts of the map forming a closure of very low, closed spaced magnetic unit to the east. The unit has a profile labelled R4 and R5 through it. The large and high anomalous unit located at the central part of the map is indicative of an emplaced plutonic rock containing magnetite. The open spaced contour on the unit is indicative of the extensive and deep-seated nature of the body.

The other magnetic units from the map are of medium and low values. The magnetic units of low anomalous values are located at the north, east and south-east. The only anomalous unit of medium value is found at the western end of the map. The profile labelled R6 to the east of the map is indicative of a very low magnetic body. The closed spaced elliptical nature of the contours is indicative of a dyke-like body whose magnetic susceptibility is very much lower than the adjacent rock body. Such rock body could be of an acidic volcanic origin in nature. The other medium magnetic unit is also elliptical in shape, however of a larger extent. It also shows a dyke body whose susceptibility is a bit higher than the one at the east. The profile labelled R3 cut across parallel contours. This area shows a fold axis or a fracture / fault zone. Such area is of significance to petroleum traps.

The lineaments trend in two major directions, which are NE- SW and NW-SE directions. The dominant trend is the NE-SW direction which is the regional trend of the Benue Trough. The NNE-SSW trend of the regional magnetic field (Fig. 5) is in conformity with the trend of the Pan-African Orogeny, a major geologic event in African.

The quantitative interpretation uses spectral analysis to evaluate the depth to the magnetic basement. In order to establish the depth to the anomalous bodies beneath, sixteen (16) rectangular cell (window) divisions were created. Spectral depth computations were made at the centre of each cell by considering the graph of the energy spectrum versus the frequency. To calculate the depth value to the basement, the slopes of the graphs were estimated, and half of the slope gives the required depth. Hence the average estimated sediment thickness for all cells is the average of the entire established half slopes through the cells.

From Table 2 the maximum half slope D_{max} which represents deeper sources ranges between 8 km and 12 km, while the minimum half slope D_{min} ranges from 1 km to 4 km. By taking the average of the two halves slopes, the established sediment thickness within the entire study area was found to be between 4.6 km and 8.0 km with the overall average across the 16 cells being about 6.5 km (6490.60 m). Therefore, the average thickness of sediment through the area is not more than 7 km. This is small compared to thickness of sediment in the Niger-Delta which has been accumulating on average of over 10 km thick.

Table 2: Established Depth to Basement (Sediment thickness) of the study area.

Cell Plot No	Dmax (m)	Dmin (m)	Average Depth (m)	Remark
1	7806.66	1432.79	4619.73	Shallow source
2	9153.82	1825.54	5489.68	Deep source
3	12819.58	2134.41	7477	very deep source
4	10426.67	925.25	5675.96	Deep source
5	7202.81	1733.34	4468.08	Shallow source
6	12110	2562	7336	Very deep source
7	10820.96	3971.26	7396.11	Very deep source
8	11028.12	1724.82	6376.47	Deep source
9	12318.41	2377.39	7347.9	Very deep source
10	12242	2080.56	7161.28	Very deep source
11	11027.5	2137.74	6582.62	Very deep source
12	13574.5	3012.83	7856.12	Very deep source
13	11835.05	1969.78	6902.41	Very deep source
14	10330.59	2170.84	6250.71	Deep source
15	11216.59	1871.33	6543.96	Very deep source
16	12536.47	1949.78	6365.63	Deep source



Conclusion

The study area contains five magnetic units. They are classified into three groups-high, medium and low. The magnetic basement around Mmaku area is of medium to low magnetic anomalies, whereas the underlying magnetic basement that forms most part of Udi plateau is of high magnetic anomaly. This shows that the rock is richer in iron compared with the surrounding rocks and could possibly be a pluton of moderate extent and of felsic magmatic origin.

The dominant lineament trend is NE-SW. This falls in line with the regional trend of the Benue Trough. So by implication the dominant events that lead to the emplacement of the linear structures are similar to that which took place at the formative stage of the Benue Trough.

The average depth within the area is in the range of 7 km. This is a very low sediment thickness compared to the sediment thickness in the Niger-Delta region which is over 10 km and still accumulating. However, the 7 km depth is sufficient for hydrocarbon generation.

References

- [1]. Nabighian M. N, Grauch V. J. S, Hansen R. O, LaFehr T. R, Li Y, Pierce J. W, Philips J. D, Ruder M. E. (2005). The historical development of the magnetic method in exploration. *Geophysics* 70 (6), 33-61.
- [2]. Smith B. D, McCafferty, A. E and McDougal R. R. (2000). Utilization of airborne magnetic, electromagnetic, and radiometric data in abandoned mine land investigations: in Church, S.E., ed., Preliminary release of scientific reports on the acidic drainage in the Animas River watershed, San Juan County, Colorado: U. S. Geological Survey Open File Report 00-0034, 86-91.
- [3]. Blakely R. J, Langenheim V.E, Ponce D. A and Dixon G. L. (2000a). Aeromagnetic survey of the Amargosa Desert, Nevada and California; a tool for understanding near-surface geology and hydrology: U. S. Geological Survey Open File Report 00-0188, available online at <http://geopubs.wr.us.gov/open-file/of00-188/>.
- [4]. Saltus R.W, Haeussler P. J, and Phillips J. D. (2001). Geophysical mapping of subsurface structures in the upper Cook Inlet basin, Alaska: Geological Society of America Abstracts with Programs, 33, 345-359.
- [5]. Langenheim V. E, Jachens R. C, Morton D. M, Kistler R. W and Matti J. C. (2004). Geophysical and isotopic mapping of pre-existing crustal structures that influenced the location and development of the San Jacinto fault zone, southern California: Geological Society of America Bulletin, 116, 1143-1157.
- [6]. Finn C. A, Sisson T. W and Deszcz-Pan M. (2001). Aerogeophysical measurements of collapse-prone hydrothermally altered zones at Mount Rainier Volcano: *Nature*, 409, 600-603.
- [7]. McConnell T. J, Lo B, Ryder-Turner A and Musser J. A. (1999). Enhanced 3D seismic surveys using a new airborne pipeline mapping system: SEG Expanded Abstracts, 18, 516-519.
- [8]. Tsokas G. N and Papazachos C. B. (1992), Two-dimensional inversion filters in magnetic prospecting: Application to the exploration for buried antiquities: *Geophysics*, 57, 1004-1013.
- [9]. Campos-Enriquez J. O, Diaz-Navarro R, Espindola J. M and Mena M. (1996). Chicxulub - Subsurface structure of impact crater inferred from gravity and magnetic data: *The Leading Edge*, 15, 357-359.
- [10]. Goussev S. A, Charters R. A, Peirce J. W and Glenn W. E. (2003). The Meter Reader - Jackpine magnetic anomaly: Identification of a buried meteorite impact structure: *The Leading Edge*, 22, 740-741.
- [11]. Nettleton L. L. (1971). Elementary Gravity and Magnetism for geologists and seismologists. Society of Exploration Geophysicists, Monograph series, no. 1, 121p.
- [12]. Reynolds L. R, Rosenbaum J. G, Hudson M. R and Fishman N. S. (1990). Rock Magnetism, the distribution of magnetic minerals in the earth crust and aeromagnetic anomalies: U.S. Geological Survey and aeromagnetic anomalies: U.S. Geological Survey, Bulletin 1924, 24-45.
- [13]. Grauch V. J. S and Milleagan P. S. (1998). Mapping intrabasinal faults from high-resolution aeromagnetic data: *The Leading Edge*, 17 (1). 53-55.



- [14]. Oyebuchi A. R. (2011). Interpretation of Aeromagnetic and Landsat Imageries of Okposi, Ebonyi State, SE Nigeria (Unpub. M.Sc Thesis, Uniport). 116p.
- [15]. Okogbue C. O. (2006). Hydrocarbon potential of the Anambra basin: Geology, Geochemistry and Geohistory perspective. Great Ap express Pub., Ltd.
- [16]. Murat R. C., (1972). Stratigraphy and paleogeography of the Cretaceous and lower Tertiary in southern Nigeria. In Dessauvage, T.F.J and Whiteman, A. J., (Eds.), African Geology. University of Ibadan Press, 251-266.
- [17]. Reeves C. (2005). Aeromagnetic surveys: principles, practice and interpretation. Geosoft Pub. 155p.
- [18]. Spector, A., and Grant, F. S., (1970). Statistical models for interpreting aeromagnetic data: Geophysics, v. 35, 293-302.

